



Piezoelectric Photoacoustic System for Fluid Flow Monitoring

Hui Ling Chua¹, Audrey Huong^{2*}

¹Department of Electrical and Electronic Engineering, Faculty of Electrical and Electronic Engineering, Universiti Tun Hussein Onn Malaysia, Parit Raja, 86400, MALAYSIA

²Department of Electrical and Electronic Engineering, Faculty of Electrical and Electronic Engineering, Universiti Tun Hussein Onn Malaysia, Parit Raja, 86400, MALAYSIA

*Corresponding Author

DOI: <https://doi.org/10.30880/ijie.2020.12.07.023>

Received 3 September 2020; Accepted 12 October 2020; Available online 31 October 2020

Abstract: The aim of this study is to investigate the feasibility of using a laboratory assembled piezoelectric based photoacoustic (PA) system for noncontact monitoring fluid flow. This is to overcome the drawbacks of some existing fluid flow detection systems, which include expensive equipment and their maintenance cost, limited sensitivity and specificity in detecting signals from restricted regions or at low flow velocity. The produced PA signal waves detected by a piezoelectric transducer used in this study was processed to determine the required phase value (Φ), which value was found to correlate linearly with fluid flow status. The fluid pressure difference of 1.16 pascals (Pa) and 11.90 Pa applied to the developed mock circulatory system was observed to produce changes in phase value with mean \pm standard deviation (SD) $\Delta\Phi$ of 0.79 ± 0.07 rad and 2.17 ± 0.07 rad, respectively, suggesting a linear response of the developed system with changes in circulation system. This trend was supported with the relatively low absolute difference of 0.07 ± 0.01 rad in the predicted values as compared to that of the ground truth. This work concluded that the capabilities and simplicity of the proposed PA system renders it feasible for cost effective, non-destructive assessment of fluid flow in future studies.

Keywords: Photoacoustic imaging, fluid flow, phase value, phase difference

1. Introduction

Flow measurement is a process of quantifying fluid movement. The water meter, which was first used 3000 years ago by the Egyptians for prediction of their land fertility was a crude form of weir [1]. To date, fluid dynamics can be measured by using a variety of devices such as ultrasonic flowmeter, anemometer, positive-displacement flow meters and others [2-4]. Accurate measurement of fluid and gas flow is crucial to ensure the efficiency and effectiveness of systems in diverse applications that require continuous monitoring of mass flow measurement, such as at power plants of natural gas, compressed air, steam generator and water supply, and to test boiler efficiency. This is especially useful to determine the fluid or gas consumption and for leakage detection. Joshi *et al.* [5] reported an innovative flow sensor consists of a surface acoustic wave (SAW) oscillator, which is heated to a suitable temperature above the ambient before its operation. The convective cooling caused by fluid flow decreases the substrate temperature, thereby causing a change in the oscillator frequency; this gives rise to a direct measurement system with high sensitivity and excellent dynamic range, which digital output is related linearly to the measured acoustic waves. Acoustic waves are a type of energy propagation through a medium with a unique characteristic acoustic velocity. The acoustic based technology has been adopted in various equipment including ultrasound machines and ultrasonic receiver (e.g. EPOCH 650) for non-destructive monitoring and diagnosis purposes. The latter system is the most recent ultrasonic sensor that is able to provide phase measurement of a signal. Among the works that made use of EPOCH 650 in their system include Hariri

*Corresponding author: chua865@gmail.com

et al. [6] for measurement of biologically features of tissues, wherein mechanical structure of tissues can be identified based on their acoustic properties depending on viscosity of the sample.

Similar to acoustic waves, its counterpart photoacoustic (PA) waves is the sound waves produced in the presence of optical source, which operation is based on the optical-acoustic effect. Non-ionizing light source delivers light energy to an investigated medium, medium's absorber(s) would absorb the photonic energy and start to vibrate. Thermal expansion occurred during the light energy absorption results in ultrasonic emission (i.e. PA generation), which magnitude is proportional to the energy absorbed. This could be used to reveal the specific optical absorption of sample absorber(s). A work by Viegrov [7] demonstrated the use of photoacoustic spectroscopy (PAS) that adopted PA technology to determine gas concentration in a mixed gas, since then this system has found its application in numerous investigations of gaseous samples [8, 9]. In addition PA approach is shown to exhibit a great potential in preclinical research, clinical and diagnostic practice [10] to provide both structural and functional optical information of biological tissues with high spatial resolution as compared to ultrasound technique. The result generated from PA system depends not only on mechanical and elastic properties of the tissue but also its optical absorption properties. This technique is suitable for real time and non-invasive monitoring of biomedical function and dynamic without involving ionizing radiation. In addition to the investigation of anatomical structures such as the microvasculature, this technique is able to provide functional information of human body such as blood oxygenation, blood flow and temperature [11-13].

Blood circulation is one of the most important functions in a living organism's body to deliver blood carrying oxygen to the brain and other organs. It can also promote healthier skin and help with cell growth. Sound waves have been used extensively in the study of circulatory disorders [14, 15]. Arteriosclerosis is one of these disorders, which often begins with injury to the endothelium of an artery. The latter may be caused by infection, excessive lipids and fats in the tissues and high blood glucose level. These circulating lipoproteins may accumulate within the arterial wall and turning into plaque, which narrows the arterial lumen and resists the blood flow. Vessel narrowing leads to ischemia and hypoxia that may severely impair brain and heart function. Previous researchers [16-18] reported the feasibility of using acoustic waves to detect coronary stenosis based on the discernable sounds produced by the heart. However the current imaging systems such as color flow imaging, which exploits the measured time and phase shift to estimate the axial component of the blood flow, can be of complex and costly construction [19]. The use of these imaging systems is limited by their low measurement sensitivity at low flow rate [20], which often leads to the use of contrast agents for enhance visualization [21-23]. Meanwhile Murphy *et al.* [24] showed that eventhough power Doppler imaging, a new sonographic technique, can be suitably used to evaluate the performance of vascular system i.e. amplitude or strength of the Doppler signal to distinguish small vessels and slow moving blood, it is not able to reveal directional information. This work aims to investigate the feasibility of an assembled piezoelectric based PA system for label-free fluid flow monitoring via comparison using Olympus ultrasonic receiver (EPOCH 650).

2. Material and method

Light waves of center wavelength, λ , 633 nm produced by a continuous laser source (R-30993, Newport Corp.) shown in Fig. 1 were allowed to pass through an acousto-optic modulator (AOM) controlled by a radiofrequency (RF) driver to produce trains of laser pulses of frequency 80 MHz required for the generation of thermal expansion within the investigated sample. The arrangement and details of this modulation system can be found in our previous work [25]. The temperature variation in the medium produces sound waves (photoacoustic signals) of different vibrational velocity, which amplitude is proportional to the energy of the laser beam absorbed, was measured using an unfocused piezoelectric transducer (model: LF 2000K1, 2 MHz). The latter was connected to an oscilloscope (model: Rohde & Schwarz – HMO2022) for acquisition and storing of data. The PA results are then analyzed and compared with that provided by EPOCH 650, which is taken here as the ground truth, for the evaluation of system performance.

2.1 Phantom microcirculatory system

Microcirculatory is a system that allows blood to circulate and deliver nutrients, oxygen, hormones and other gaseous to and from cells within the body systems to maintain homeostasis. Blood vessel larger than 10 mm in diameter is regarded as elastic [26] as it allows the vessel to expand for better pumping of blood, and diameter of arteries typically ranged from 0.1 mm to 10 mm depending on its location within the body system [27]. A phantom system that simulates human microcirculatory shown at the center of Fig. 1 was prepared for investigation work. This system used polyethylene (PE) tube to represent elastic blood vessel, while water pump is to mimic heart contraction to pump blood into the entire system. Water was used as a substitute of blood in this study largely due to the high similarity in their medium density, which renders the former commonly used in studies to verify intraoperative blood loss [28]. The different flow rate along the PE tube was achieved by applying different voltage to a waterproof water pumping system (model. JT-180A) shown on the right of Fig. 1 to produce relatively constant flow velocity ranges from 1.67 to 5.83 litre/minutes detectable by a water flow sensor (YF-S401). Also shown in Fig. 1 is the placement of transducer for measurement of PA waves following the supplied voltage level. This phantom circulation system was drawing power from a direct-current (DC) power supply (SKU-878306) controlled using Arduino Uno (Rev 3). This

system costs around USD 9,000 (MYR 38,450) in material for construction, which is considered cheaper as compared to the market available devices such as EPOCH 650.

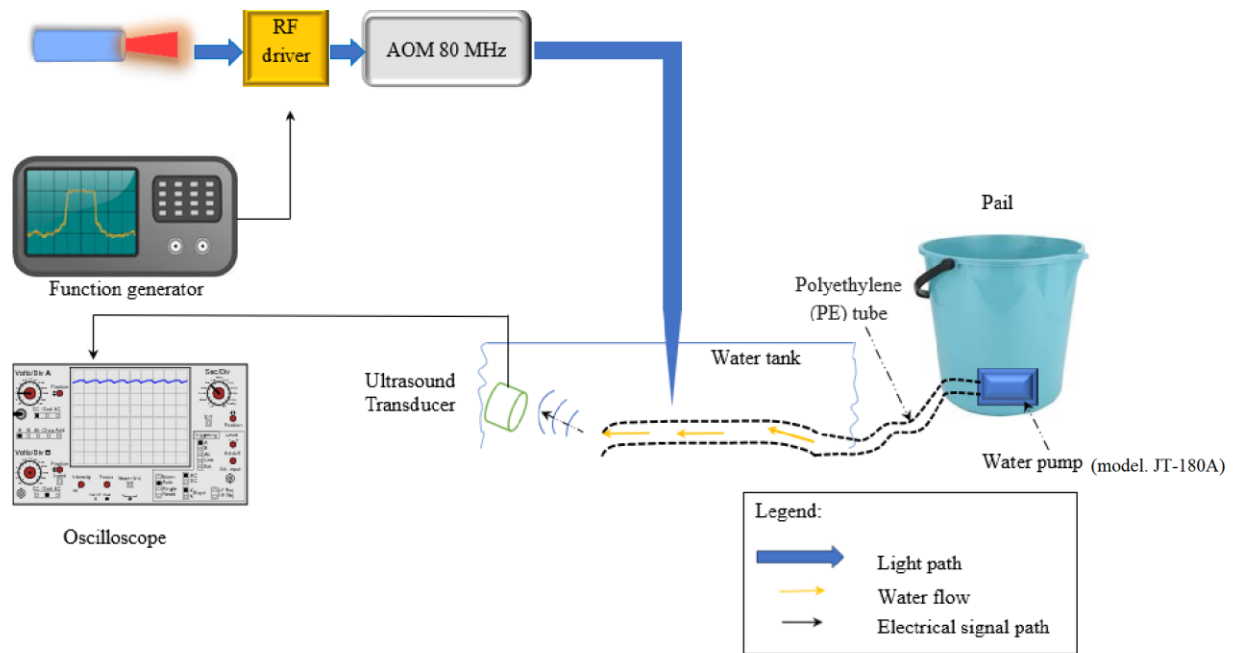


Fig. 1 - Schematic diagram of photoacoustic (PA) imaging system

2.2 Fluid flow control system

A DC voltage supply was used to produce pressure drop across the PE tube via a water pump. The supplied voltage level was arbitrarily selected as 4.5 V, 6 V, 9 V and 12 V. Each of the voltage level produces different fluid rate flowing through the PE tube. Three sets of data were consecutively collected for each experiment, from which mean and standard deviation (SD) are calculated. The relationship between the peak magnitude of the measured PA value in units of volts (mV) following the exerted fluid pressure, P , is given as followed [29, 30]:

$$P = \frac{V}{\rho} \tag{1}$$

where V and ρ represent the measured peak PA value and total fluid volume, respectively. The differences in the supplied voltage (V_1 and V_2) mentioned in earlier paragraph give rise to the change in fluid pressure (ΔP) in units of pascals (Pa) of 1.16, 5.88, 11.90, 3.53, 9.52 and 4.76 shown in Table 1.

Table 1 - Changes in fluid pressure (ΔP) induced by different voltage supplied to phantom circulation system

Supplied voltage (V)		Difference in fluid pressure, ΔP (Pa)
V_1	V_2	
4.5	6	1.16
	9	5.88
	12	11.90
6	9	3.53
	12	9.52
9	12	4.76

2.3 Signal processing and analysis

This study used Fast-Fourier transform (FFT) function available in MATLAB (version 2016a) in (2) for conversion of time-dependent signals to frequency domain. The PA signals detected by the piezo-transducer give real (Ψ_{re}) and imaginary (Ψ_{im}) components of the measured voltage, which represents signal attenuation and echoes, respectively. The analogue signals are then digitized for FFT analysis. The phase value, Φ , in units of radians (rad) calculated from the components of PA signals in (3) is shown in (4). The value for real and imaginary part of PA signals are inversely proportional to each other [31]. It should be mentioned that phase value is corresponded to the amplitude of PA signal detected by transducer, wherein the higher the amplitude the more light absorption by absorber(s) within the medium [31, 32].

$$(\Psi_{re}, \Psi_{im}) = FFT(\psi(t)) \tag{2}$$

where $\psi(t)$ represents acoustic wave in time domain. Next, phase difference, $\Delta\Phi$ (rad), is calculated from Eq. (4) to determine the difference in the FFT peak of two acoustic signals (e.g. signal x , y) produced following the supply of V_1 and V_2 in Table 1, respectively.

$$\Phi = \tan\left(\frac{\Psi_{im}}{\Psi_{re}}\right) \tag{3}$$

$$\Delta\Phi = \Phi_{(y)} - \Phi_{(x)} \tag{4}$$

3. Results and analysis

The measured time dependent PA signals for different applied voltage of 6 V and 9 V is shown in Fig. 2. Fig. 3 shows changes in the calculated fluid pressure with differences in the supplied voltage based on the values tabulated in Table 1. Meanwhile $\Delta\Phi$ following changes in different fluid pressure calculated in (4) is shown in Fig. 4.

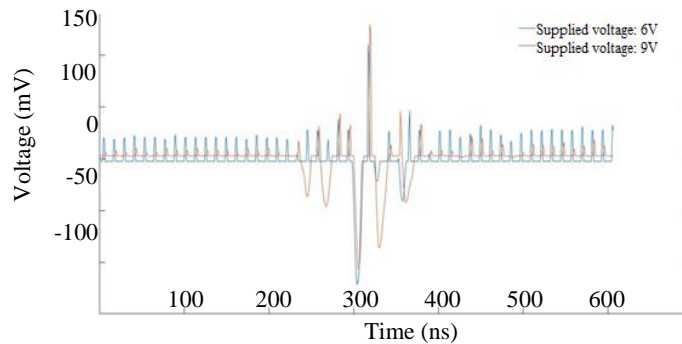


Fig. 2 - The measured time dependent PA signals for different voltage supplied to phantom microcirculatory system

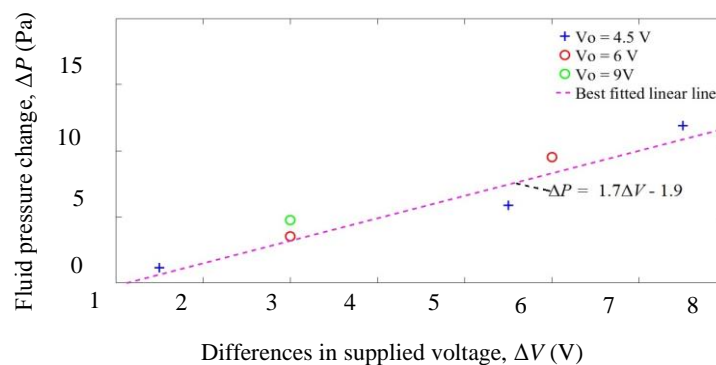


Fig. 3 - Fluid pressure change, ΔP , with changes in voltage supplied, ΔV , to the circulation system

The diagram shows mean and standard deviation, SD, (shown as magnitude of errorbars) of changes in phase value (from three consecutive experiments) with the supplied voltages. The fluid pressure ranges from 1.16 pascals (Pa) to 11.90 Pa applied to the developed mock circulatory system was found to produce a notably linearly increase in $\Delta\Phi$ from 0.79 ± 0.07 rad to 2.17 ± 0.07 rad, suggesting a linear response of the developed system with changes in circulation system.

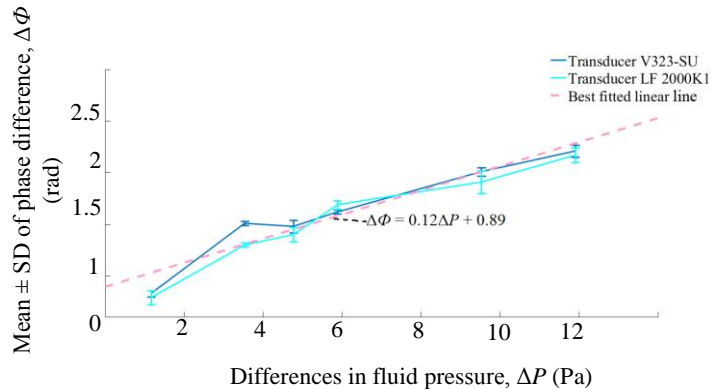


Fig. 4 - Mean and standard deviation (SD) of calculated phase difference with variation in fluid pressure

Also shown in Fig. 4 is the results obtained from the EPOCH 650 using V323-SU transducer. Based on the results in Fig.4, the absolute difference in the predicted $\Delta\Phi$ and that given from the EPOCH 650 system is calculated as 0.07 ± 0.01 rad.

4. Discussion and conclusion

The results in Fig. 3 showed that fluid pressure change is linearly proportional to the differences in the supplied voltage, which can be represented by a linear function. This suggests a linear response of the developed system with changes in circulatory performance. The slight difference in fluid pressure change at ΔV of 3 V in Fig. 3 (i.e. produced by voltage supply of 6 V - 9 V pair and 9 V - 12 V pair in Table 1) revealed two different ΔP values of 3.53 Pa and 4.76 Pa. This inconsistency may possibly be explained by the different shear rate produced by the applied voltage, supported by the fact that water is a Newtonian fluid, which viscosity is independent of shear rate [33]. Here an increase in voltage supply, and hence medium pressure, promotes higher shear rate and encourages fluid flow velocity [34-37]. Therefore the supplied 9V - 12 V difference is able to generate a higher shear strength as compared to their counterpart.

Since both piezo-PA and EPOCH system adopt piezo technology in their systems, Fig. 4 showed an increasing trend of similar magnitude in the calculated phase change with fluid pressure difference detected by both systems. EPOCH system uses piezoelectric ceramic transducer (i.e. a micro-machined element of piezoelectric ceramic embedded in an epoxy matrix). This composite element with enhanced detection bandwidth improves sensitivity in flaw detection [38]. This results in a better receptive and accuracy in the system to the measurement of fluid flow as compared to the constructed system. It must also be mentioned that the results may be varied with the different transducer (detection) beam patterns. Since EPOCH system is able to focus spherically (spot) and cylindrically (line), this allows it to record a more concentrated PA signals as compared to the unfocused linear transducer used in the developed system. Nonetheless the remarkably low absolute difference in ΔP of 0.07 ± 0.01 Pa between these systems in Fig. 4 supports the feasibility of using the developed system for the measurement of fluid flow status.

Although Fig. 2 showed a visually indistinguishable pattern of PA signals, the analytical techniques applied on the signals as discussed in section 2.3 allow us to discern changes in fluid flow. The linear change in phase difference with the fluid pressure observed in Fig. 4 agreed well with the principle of Doppler shift [39-43]. Doppler effect causes a linear change in frequency of an incident wave with the difference in velocity between the transmitter and receiver [44], and phase change of a cycle in a period of time is equivalent to a Doppler shift of frequency. This study concluded that even though the values and relationship observed in Fig 3 and Fig. 4 are valid for the employed experimental system and conditions presented herein, the results showed the feasibility of the developed system for noninvasive assessment of fluid flow with acceptable performance, implying its potential application as a label-free technology at a fractional price compared to market available system (e.g. EPOCH 650). The future of this work includes the use of this piezo-photoacoustic system for *in-vivo* study of human tissues, such as hydration level and hemoglobin binding status by exploiting the different PA properties of the underlying chromophores.

Acknowledgement

We are grateful to Universiti Tun Hussein Onn Malaysia under GPPS Grant Vot Number H302 for financially supporting this work.

References

- [1] F. Cascetta. (1995). Short history of the flowmetering. *Isa Transactions*, 34, 229-243
- [2] J. Woodcock (1975). Development of the ultrasonic flowmeter. *Ultrasound in medicine & biology*, 2, 11-18
- [3] P. K. Paulsen (1980). The Hot-Film Anemometer—a Method for Blood Velocity Determination. *European Surgical Research*, 12, 149-158
- [4] B. Wijay and P. Angelini, Positive displacement piston driven blood pump. ed: Google Patents, 1991
- [5] S. G. Joshi. (1994). Flow sensors based on surface acoustic waves. *Sensors and Actuators A: Physical*, 44, 191-197
- [6] A. Hariri, M. Hosseinzadeh, S. Noei, and M. Nasirivanaki (2017). Photoacoustic signal enhancement: towards utilization of very low-cost laser diodes in photoacoustic imaging. *Photons Plus Ultrasound: Imaging and Sensing 2017*, 100645L
- [7] M. Viegerov (1938). Eine Methode der Gasanalyse, Beruhend auf der Optisch-Akustischen Tyndall-Röntgenerscheinung. *Dokl. Akad. Nauk SSSR*, 687-688
- [8] T. Tomberg, M. Vainio, T. Hieta, and L. Halonen (2018). Sub-parts-per-trillion level sensitivity in trace gas detection by cantilever-enhanced photo-acoustic spectroscopy. *Scientific reports*, 8, 1-7
- [9] H. Wu, L. Dong, H. Zheng, Y. Yu, W. Ma, L. Zhang, et al. (2017). Beat frequency quartz-enhanced photoacoustic spectroscopy for fast and calibration-free continuous trace-gas monitoring. *Nature communications*, 8, 1-8
- [10] J. Xia, J. Yao, and L. V. Wang (2014). Photoacoustic tomography: principles and advances. *Electromagnetic waves (Cambridge, Mass.)*, 147, 1
- [11] J. Shah, S. Park, S. R. Aglyamov, T. Larson, L. Ma, K. V. Sokolov, et al. (2008). Photoacoustic imaging and temperature measurement for photothermal cancer therapy. *Journal of biomedical optics*, 13, 034024
- [12] J. Laufer, D. Delpy, C. Elwell, and P. Beard (2006). Quantitative spatially resolved measurement of tissue chromophore concentrations using photoacoustic spectroscopy: application to the measurement of blood oxygenation and haemoglobin concentration. *Physics in Medicine & Biology*, 52, 141
- [13] M. Schwarz, A. Buehler, J. Aguirre, and V. Ntziachristos (2016). Three-dimensional multispectral optoacoustic mesoscopy reveals melanin and blood oxygenation in human skin in vivo. *Journal of biophotonics*, 9, 55-60
- [14] A. Cassone. Method for treating circulatory disorders with acoustic waves. ed: Google Patents, 2002.
- [15] R. Nagaoka, K. Sasaki, S. Zama, M. Nagone, H. Nagai, Y. Takeuchi, et al. (2016). Perspective imaging of flow in arterial model obtained with continuous wave Doppler focusing technique. 2016 38th Annual International Conference of the IEEE Engineering in Medicine and Biology Society (EMBC), 2315-2318
- [16] L. H. Hudgins and P. A. Chandraratna. Non-invasive acoustic screening device for coronary stenosis. ed: Google Patents, 2000
- [17] W.-C. Chien, W.-M. Liu, and A.-B. Liu (2016). Envelope approximation on doppler ultrasound spectrogram for estimating flow speed in carotid artery. 2016 International Computer Symposium (ICS), 415-418
- [18] J. K. Roy, T. S. Roy, and S. C. Mukhopadhyay (2019). Heart Sound: Detection and Analytical Approach Towards Diseases. *Modern Sensing Technologies*, ed: Springer, 103-145. Hui Ling Chua et al., *Int. J. of Integrated Engineering Vol. 12 No. 7 (2020) p. 205-211* 211
- [19] J. A. Jensen, S. I. Nikolov, C. Alfred, and D. Garcia (2016). Ultrasound vector flow imaging—Part I: Sequential systems. *IEEE transactions on ultrasonics, ferroelectrics, and frequency control*, 63, 1704-1721
- [20] K. Martin. (2011). Basic equipment, components and image production. *Clinical ultrasound*, ed: Elsevier, 16- 30
- [21] C. Errico, B.-F. Osmanski, S. Pezet, O. Couture, Z. Lenkei, and M. Tanter. (2016). Transcranial functional ultrasound imaging of the brain using microbubble-enhanced ultrasensitive Doppler. *NeuroImage*, 124, 752- 761
- [22] M. Zeisbrich, L. P. Kihm, F. Drüscher, M. Zeier, and V. Schwenger. (2015). When is contrast-enhanced sonography preferable over conventional ultrasound combined with Doppler imaging in renal transplantation. *Clinical kidney journal*, 8, 606-614
- [23] A. Ignee, N. S. Atkinson, G. Schuessler, and C. F. Dietrich (2016). Ultrasound contrast agents. *Endoscopic ultrasound*, 5, 355
- [24] K. J. Murphy and J. M. Rubin. (1997). Power Doppler: it's a good thing. *Seminars in Ultrasound, CT and MRI*, 13- 21
- [25] Hui Ling Chua, Audrey Huong (2020). Photoacoustic Imaging System for Biological Tissues Characterization. *International Journal of Advanced Science and Technology*, 29, 854-859
- [26] A. Ostadfar, *Biofluid mechanics: Principles and applications*: Academic Press, 2016
- [27] Sabrina Beauvais, Olivier Drevelle, Jessica Jann, Marc-Antoine Lauzon, Mohammadreza Foruzanmehr, Guillaume Grenier4, Sophie Roux, Nathalie Faucheux (2016). Interactions between bone cells and biomaterials: An update. *Frontiers in Bioscience, Scholar*, 8, 227-263

- [28] D. J. Vitello, R. M. Ripper, M. R. Fettiplace, G. L. Weinberg, and J. M. Vitello (2015). Blood density is nearly equal to water density: a validation study of the gravimetric method of measuring intraoperative blood loss. *Journal of veterinary medicine*, 2015
- [29] I. C. Christov, V. Cognet, T. C. Shidhore, and H. A. Stone (2018). Flow rate–pressure drop relation for deformable shallow microfluidic channels. *Journal of Fluid Mechanics*, 841, 267-286
- [30] X. Cheng, X. Xue, Y. Ma, M. Han, W. Zhang, Z. Xu, et al. (2016). Implantable and self-powered blood pressure monitoring based on a piezoelectric thinfilm: Simulated, in vitro and in vivo studies. *Nano Energy*, 22, 453-460
- [31] F. Gao, R. Zhang, X. Feng, S. Liu, R. Ding, R. Kishor, et al. (2017). Phase-domain photoacoustic sensing. *Applied Physics Letters*, 110, 033701
- [32] W. Xia, D. I. Nikitichev, J. M. Mari, S. J. West, R. Pratt, A. L. David, et al. (2015). Performance characteristics of an interventional multispectral photoacoustic imaging system for guiding minimally invasive procedures. *Journal of biomedical optics*, 20, 086005
- [33] H. F. George and F. Qureshi (2013). Newton’s Law of Viscosity, Newtonian and Non-Newtonian Fluids. *Encyclopedia of Tribology*, 2416-2420
- [34] B. A. Morris, *The science and technology of flexible packaging: multilayer films from resin and process to end use: William Andrew*, 2016
- [35] D. D. Braun and M. R. Rosen, *Rheology Modifiers Handbook: Practical Use and Application: Elsevier*, 2013
- [36] R. Klabunde, *Cardiovascular physiology concepts: Lippincott Williams & Wilkins*, 2011
- [37] R. C. Penwell. *Pressure effects in the capillary flow of newtonian and shear-thinning polymers*. 1970
- [38] T. Nelligan, *An Introduction to Ultrasonic Transducers for Nondestructive Testing*. Olympus, vol. Olympus Industrial Resources
- [39] D. L. Franklin, W. Schlegel, and R. F. Rushmer (1961). Blood flow measured by Doppler frequency shift of back-scattered ultrasound. *Science*, 134, 564-565
- [40] A. A. Oglat, M. Matjafri, N. Suardi, M. A. Oqlat, M. A. Abdelrahman, and A. A. Oqlat (2018). A review of medical doppler ultrasonography of blood flow in general and especially in common carotid artery. *Journal of medical ultrasound*, 26, 3
- [41] P. Tortoli, M. Lenge, D. Righi, G. Ciuti, H. Liebgott, and S. Ricci. (2015). Comparison of carotid artery blood velocity measurements by vector and standard Doppler approaches. *Ultrasound in medicine & biology*, 41, 1354-1362
- [42] K. K. Shung, *Diagnostic ultrasound: Imaging and blood flow measurements: CRC press*, 2015
- [43] C. Deane (2015). *Doppler ultrasound: principles and practice. Placental and fetal Doppler*, ed: CRC Press, 10
- [44] M. Singh. *Ultrasonic Doppler Flowmeter -Introduction to Biomedical Instrumentation. Technology and Engineering*, 2014